after switch-off of the condensation and subsequent warm-up of the matrix.

[1] L. König, I. Rabin, W. Schulze, G. Ertl, *Science* **1996**, *274*, 1353 – 1355.

[2] R. D. Levine, R. B. Bernstein, *Molecular Reaction Dynamics and Chemical Reactivity*, **1987**, Oxford University Press, New York.

[3] A. Ben-Shaul, Y. Haas, K. L. Kompa, R. D. Levine in *Lasers and Chemical Change*, Springer Series: Chem. Phys., **1981**, Springer, Berlin, vol. 10, p. 289.

[4] M. G. Prisant, C. T. Rettner, R. N. Zare, *J. Chem. Phys.* **1984**, *81*, 2699 – 2712.

[5] I. Rabin, W. Schulze, G. Ertl, *J. Chem. Phys.* **1998**, *108*, 5137 – 5142.

[6] C. Félix, C. Siber, W. Harbich, J. Buttet, I. Rabin, W. Schulze, G. Ertl, *Chem. Phys. Lett.* **1999**, *313*, 105 – 109.

[7] C. Felix, C. Sieber, W. Harbich, J. Buttet, I. Rabin, W. Schulze, G. Ertl, *Phys. Rev. Lett.* **2001**, *86*, 2992 – 2995.

[8] V. B. Yuferov, *Sov. Phys. Tech. Phys.* **1975**, *20*, 378 – 380.

[9] H. Abe, W. Schulze, *Chem. Phys.* **1979**, *41* , 257 – 263.

[10] W. Schulze, D. M. Kolb, *J. Chem. Soc. Faraday Trans. II* **1974**, *70*, 1098 – 1105.

Optimal System Size for Mesoscopic Chemical Oscillation

Zhonghuai Hou* and Houwen Xin*[a]

When driven far from equilibrium, nonlinear chemical or biochemical reactions often show sustained oscillations.[1] Oscillation is of ubiquitous importance in nature, especially the circadian rhythmic processes in living systems.[2] On the macroscopic scale, the dynamic behavior of such systems can be described by deterministic nonlinear differential equations that govern the evolution of the chemical concentrations with time, and oscillations are often the consequence of Hopf bifurcations (HBs) with variation of some control parameters. However, it is now generally asserted that circadian rhythms are funamentally controlled by biochemical clocks, which can be observed at the single-cell level.[3] In mesoscopic systems of this type, in which the number of reactant molecules is often small, internal noise resulting from the stochastic nature of the discrete chemical reaction events becomes important.[4] The macroscopic deterministic description is no longer applicable, and this calls for the use of stochastic models such as a chemical master equation which describes the evolution with time of the probability of

having a given number of reactant molecules.[5] Therefore, a basic question is: How does the oscillatory behavior of the system change with its size?

With regard to this question, two basic points have been addressed so far. In deterministic dynamic behavior at the macroscopic limit, the parameter space of the system can be divided into two major regions: the oscillation region on one side of the HB point, and the nonequilibrium steady-state (NESS) region on the other. In the oscillation region, the regular oscillatory behavior observed at the macroscopic limit will become "stochastic" when the system is small. There is a fundamental lower limit on the system size for which the oscillations remain correlated in time.[6] Hence, the major issue in this region is the robustness or resistance of the oscillations to molecular noise due to the small system size.[7] In the NESS region, the steady state observed in the macroscopic kinetics shows considerable fluctuations when the size becomes small. Thus, for a sufficiently small system, it is hard to distinguish qualitatively between fluctuations around the NESS and stochastic oscillations, and in such a mesoscopic system there is no clear manifestation of the Hopf bifurcation in the corresponding macroscopic system.[8]

Here we report a nontrivial size effect when the system is located in the NESS region but close to the HB point designated by the macroscopic kinetics. At the macroscopic limit, the system shows a stable steady state and no sustained oscillation. When the system size decreases to the mesoscopic range, the HB becomes obscure, and "stochastic oscillations" with a certain characteristic frequency appear. If the system size further decreases, the oscillation will be fully overwhelmed by the internal noise. Therefore the signal-to-noise ratio (SNR) of the stochastic oscillation passes through a clear maximum with varying system size, that is, an "optimal system size for mesoscopic chemical oscillation". Note that this effect is quite different in nature from the recently reported phenomenon of "system size resonance",[9] in which the collective linear response of an array of coupled noisy elements to small periodic forces has a maximum for a certain intermediate number of elements. Similar optimal-size effects to that discussed here were also found in the study of collective spiking activities of assemblies of ion channels.[10, 11]

Since this behavior is quite generic and does not depend on the specific choice of reaction system, we adopted the Brusselator model for our study (similar results have also been obtained for other oscillating chemical systems and biological circadian clocks). The Brusselator model involves the reaction steps of Equation (1).[12]

$$\xrightarrow{k_1} X, \quad X \xrightarrow{k_2} Y, \quad 2X + Y \xrightarrow{k_3} 3X, \quad X \xrightarrow{k_4} \tag{1}$$
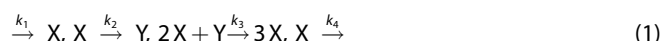
At the macroscopic limit, the deterministic reaction rate for species X and Y is given by Equation (2)

$$dx/dt = k_1 - k_2 x + k_3 x^2 y - k_4 x, \quad dy/dt = k_2 x - k_3 x^2 y \tag{2}$$

where x and y are the concentrations of X and Y, respectively. The steady-state solutions of Equation (2) are $x_s = k_1/k_4$ and $y_s = k_2 k_4/$

[a] *Prof. Z. Hou, Prof. H. Xin*
Department of Chemical Physics
University of Science and Technology of China
Hefei, Anhui, 230026 (P.R. China)
E-mail: hzhlj@ustc.edu.cn

k_1k_3. By defining a control parameter $\alpha \equiv 2k_4/k_2$, the Hopf bifurcation point $\alpha_c = 2(1 - x_s/y_s)$ is easily found, and the oscillation region is $\alpha < \alpha_c$.

If the system size is small, however, the internal molecular noise must be taken into account. Now we can describe the chemical reaction system as a birth/death stochastic process governed by a chemical master equation. Generally, there is no procedure to solve this master equation analytically, but it provides the starting point for numerical simulation. A widely used simulation algorithm was introduced by Gillespie,[13] which stochastically determines which is the next reaction step and when it will occur according to the transition probability of each reaction process in Equation (1). These transition probabilities read as in Equation (3)

$$a_1 = k_1 \cdot V, \; a_2 = k_2 x \cdot V, \; a_3 = k_3 x^2 y \cdot V, \; a_4 = k_4 x \cdot V \tag{3}$$

where V is the volume of the system. This simulation method is *exact* because it exactly accounts for the stochastic nature of the reaction events, but it is rather time-consuming and hardly applicable if the system size is large. Recently, Gillespie developed the τ-leap method, which is a rather good approximation of the exact method when the system size is large enough.[14] This method randomly determines how many steps will take place for each of the four reaction channels in the next "macro-infinitesimal" time interval τ. Therefore, we use the exact method for $V \leq V_c$ and the τ-leap method for $V \geq V_c$ in our stochastic simulations. We chose $V_c = 3 \times 10^4$ and $\tau = 0.001$ to ensure that the conditions for the τ-leap approximation were fulfilled and the simulation was effectively accelerated. For these choices of parameters, none of the propensity functions $a_j(t)$ will suffer appreciable (macroscopically noninfinitesimal) changes such that $|a_j(t+\tau) - a_j(t)|/\max_{j' \in [1,4]}[a_{j'}(t)] \ll 1$ and the number of reaction events for each channel is much greater than one.[14]

For convenience, we use α, and k_1 as the parameters instead of k_1, k_2, k_3, and k_4. We set $k_1 = 10.0$, $x_s = 1.0$, $y_s = 2.0$, and $\alpha = 1.1$, which is slightly larger than the HB value $\alpha_c \equiv 2(1 - x_s/y_s)$. At the macroscopic limit, the deterministic steady state of the system is a stable node. When the system size decreases, small fluctuations around the steady state are observed. If the system size is small enough, these fluctuations become "stochastic oscillations" for which a clear peak appears in the power spectrum of the time series $x(t)$. The frequency at the peak is very close to the characteristic frequency at the Hopf bifurcation. In Figure 1, the power spectrum of $x(t)$ for three different system sizes is plotted. Note that the smoothed curves are obtained by nearest averaging over 50 points from the original ones. The time series used to calculate the power spectrum contains 16 384 data points with an average time interval of 0.02. A Welch window function was used in the estimation of the power spectrum.[15] When the system size decreases from 10^9 to 100, one finds that both the signal level and noise background increase at the peak. However, for an intermediate system size of $V = 10^5$, the peak is the most pronounced, and this suggests the best performance of the stochastic oscillation among the three.

To measure the relative performance of the stochastic oscillation quantitatively, we defined an effective SNR as
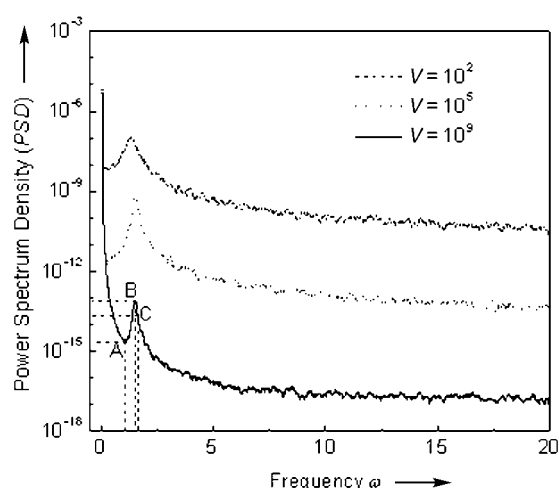
Figure 1. Smoothed power spectrum for $V = 100$, 10^5, and 10^9. Parameters are $k_1 = 10.0$, $x_s = 1.0$, $y_s = 2.0$, and $\alpha = 1.1$. The curve for $V = 100$ was obtained by the exact-simulation method, while the other two were obtained by the τ-leap method. The points A, B, and C in the PSD curve for $V = 10^9$ demonstrates how to calculate the effective SNR, that is, $\beta = [P(B)/P(A)]\omega_B/(\omega_C - \omega_B)$, where point C is located by the condition $P(C) = P(B)/e$. Arbitrary units are used for the PSD.

$\beta = R/(\Delta\omega/\omega_p)$,[16] where ω_p is the frequency at the peak, $\Delta\omega$ is the width between ω_p and the frequency ω_l satisfying $\omega_l < \omega_p$ and $P(\omega_l) = P(\omega_p)/e$, where $P(\omega_i)$ denotes the power spectrum density (PSD) for a given frequency; $R = P(\omega_p)/P(\omega_2)$, where $P(\omega_2)$ is the smallest PSD value between $P(0)$ and $P(\omega_p)$. See also the legend Figure 1 for more details. The dependence of β on system size is plotted in Figure 2a. A clear maximum is present for system size $V \approx 10^4 - 10^5$, which demonstrates the existence of an optimal system size.

Although the exact-simulation and τ-leap methods provide a direct way to study the effect of system size, they are not particularly efficient. For example, if we want to study the dynamic behavior of many coupled chemical oscillators, both methods will encounter major difficulties. Very recently, Gillespie proposed that the dynamics of the system can be approximated very well by a chemical Langevin equation (CLE) if a "macro-infinitesimal time interval" exists.[17] Specifically, the CLE for the Brusselator reads as in Equations (4)

$$dx/dt = (k_1 - k_2 x + k_3 x^2 y - k_4 x) + [\sqrt{k_1}\xi_1(t) - \sqrt{k_2 x}\xi_2(t) + \sqrt{k_3 x^2 y}\xi_3(t) - \sqrt{k_4 x}\xi_4(t)]/\sqrt{V} \tag{4a}$$

$$dy/dt = (k_2 x - k_3 x^2 y) + [k_2 x \xi_2(t) - k_3 x^2 y \xi_3(t)]/\sqrt{V} \tag{4b}$$

where $\xi_{i=1-4}(t)$ are Gaussian white noises with $\langle \xi_i(t) \rangle = 0$ and $\langle \xi_i(t)\xi_j(t') \rangle = \delta_{ij}\delta(t - t')$. In the absence of the terms in the second parenthetical expression, this CLE corresponds to deterministic Equation (2). These terms result from the internal noises, which tend to zero when the system size V goes to infinity. Note that the internal-noise terms depend not only on V, but also on the control parameters and the state variables $x(t)$ and $y(t)$. By numerical simulation of the CLE, one can readily study the effect of system size. As in the stochastic simulations, we fixed the control parameters just outside of the deterministic oscillation
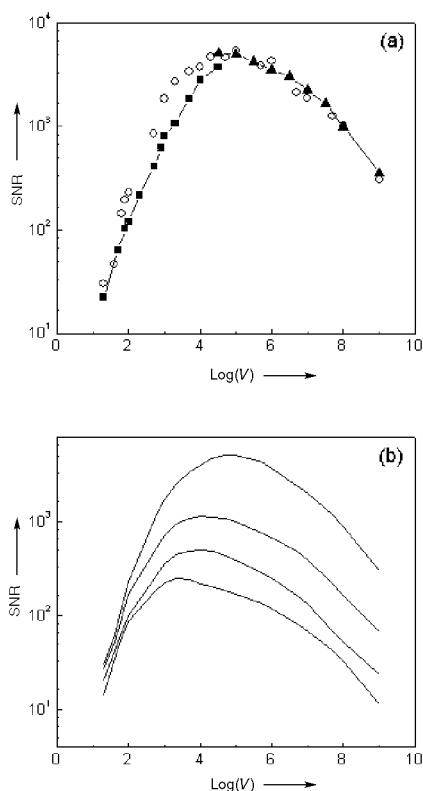
Figure 2. a) Dependence of SNR on system size V. Diamonds: Exact simulation results for $V \leq 3 \times 10^4$; triangles: τ-leap results for $V \geq 3 \times 10^4$; open circles: CLE results. All data are averaged over ten independent runs. The parameters are the same as in Figure 1. b) Dependence of SNR on system size for different α. From top to bottom, α = 1.1, 1.2, 1.3, and 1.4, respectively. The results were obtained by the CLE method, and the data have been smoothed.

region. The numerical time step was dt = 0.001. When the system size decreases from infinity, stochastic oscillations, first favored and then overwhelmed by the internal noise, are observed. The dependence of SNR on V is also plotted in Figure 2a. Good qualitative agreements among the CLE, exact-simulation, and τ-leap methods are apparent, except for some quantitative discrepancies. This agreement suggests that it is convenient to use the CLE to study the effect of system size in a systematic way. In Figure 2b, the dependence of SNR on the system size for four different values of α is plotted. When the distance from the deterministic HB point increases, both the maximal SNR and the optimal size become smaller.

This "optimal system size" effect demonstrates the important role of internal noise in chemical reaction systems. From the CLE, one notes that the internal noise term is inversely proportional to $\sqrt{V}$ if all other control parameters are fixed. Therefore, an optimal system size implies an optimal level of internal noise. This constructive role of internal noise is reminiscent of the well-known phenomenon of stochastic resonance (SR).[18] Specifically, it was found that when an excitable or oscillatory system is subjected to external noise near the Hopf bifurcation, noise-induced oscillations (NIO) are observed, and the SNR of the NIO shows a maximum at an optimal noise intensity, known as coherent resonance (CR)[17] or internal signal stochastic resonance (ISSR).[19] However, unlike CR or ISSR, one should not say

that the oscillation is "induced" by internal noise in a mesoscopic system; rather, the chemical oscillation is itself stochastic, and there is no well-defined bifurcation to separate an oscillation region from a steady-state region.

The present work may be of important relevance to circadian rhythmic processes in living systems. Since these processes are often regulated at the level of single cells, many studies now focus on their robustness and resistance to molecule noise,[6–7] in the sense that these oscillations may persist over a quite large parameter range and when some key components only have very low molecular populations. Based on the results of the present paper, however, one may understand this phenomenon from another point of view. Instead of trying to resist the internal molecular noise, living systems may have learned to exploit the internal noise to enlarge their parameter ranges of oscillation and enhance the oscillation performance.[20]

The discovery of optimal-system-size behavior may open wide perspectives for further research. For instance, consider the collective dynamic behavior of an array of coupled biochemical oscillators such as living cells. It is now widely accepted that external noise can considerably favor the collective behavior of such coupled nonlinear oscillators.[21] What happens if each cell is of mesoscopic size such that internal noise must be taken into account? Could it be that processes such as signal propagation, synchronization, and coherent motion may perform best when each cell has an optimal size? The answers to these questions deserves more detailed work in the future.

In conclusion, we have studied the effect of system size on the chemical oscillation of the Brusselator model using stochastic simulation and chemical Langevin equation. We show that a system with mesoscopic size may show sustained stochastic oscillations while its macroscopic counterpart only has a stable steady state. In addition, the performance of the oscillation, measured by the effective signal-to-noise ratio, reaches a maximum for an intermediate system size, that is, a demonstration of the phenomenon of "optimal system size for mesoscopic chemical oscillation". Our findings may be of important relevance to circadian rhythmic processes in living systems.

Acknowledgements

[1] Y. Kuramoto, *Chemical Oscillations, Waves and Turbulence*, Springer-Verlag, Berlin, Heidelberg, **1984**.
[2] A.Goldbeter, *Nature* **2002**, *420*, 238 – 245.
[3] J. C.Dunlap, *Cell* **1999**, *96*, 271 – 290.
[4] N. Barkai, S. Leibler, *Nature* **2000**, *403*, 267 – 268.
[5] N. G. Van Kampen, *Stochastic Processes in Physics and Chemistry*, North-Holland Publishing Company, Amsterdam, **1981**.
[6] D. Gonze, J. Halloy, P. Gaspard, *J. Chem. Phys.* **2002**, *116*, 10 997 – 11 010.
[7] D. Gonze, J. Halloy, A. Goldbeter, *Proc. Natl. Acad. Sci. USA* **2002**, *99*, 673 – 678; J. M. G. Vilar, H. Y.Kueh, N.Barkai, S.Leibler, *Proc. Natl. Acad. Sci. USA* **2002**, *99*, 5988 – 5992.

[8]   H. Qian, S. Saffarian, E. L. Elson, *Proc. Natl. Acad. Sci. USA* **2002**, *99*, 10 376 – 10 381.

[9]   A. Pikovsky, A. Zaikin, M. A. de la Casa, *Phys. Rev. Lett.* **2002**, *88*, 050601.

[10] G. Schmid, I. Goychuk, P. Hänggi, *Europhys. Lett.* **2001**, *56*, 22 – 28.

[11] P. Jung, J. Shuai, *Europhys. Lett.* **2001**, *56*, 29 – 35.

[12] P. Gaspard, *J. Chem. Phys.* **2002**, *117*, 8905 – 8916.

[13] D. T. Gillespie, *J. Phys. Chem.* **1977**, *81*, 2340 – 2361.

[14] D. T. Gillespie, *J. Chem. Phys.* **2001**, *115*, 1716 – 1733; D. T. Gillespie, and L. R. Petzold, *J. Chem. Phys.* **2003**, *119*, 8229 – 8234.

[15] W. H. Press, S. A. Teukolsky, W. T. Vetterling, B. P. Flannery, *Numerical Recipes in C*, 2nd Ed., Cambridge University Press, New York, **1992**.

[16] H. Gang, T. Ditzinger, C. Z. Ning, H. Haken, *Phys. Rev. Lett.* **1993**, *71*, 807 – 810.

[17] D. T. Gillespie, *J. Chem. Phys.* **2000**, *113*, 297 – 306.

[18] L. Gammaitoni, P. Hänggi, P. Jung, F. Marchesoni, *Rev. Mod. Phys.* **1998**, *70*, 223 – 285; P. Hänggi, *ChemPhysChem* **2002**, *3*, 285 – 290.

[19] Z. H. Hou, H. W. Xin, *Phys. Rev. E* **1999**, *60*, 6329 – 6332.

[20] C. V. Rao, D. M. Wolf, A. P. Arkin, *Nature* **2002**, *420*, 231 – 237.

[21] C. S. Zhou, J. Kurths, B. B. Hu, *Phys. Rev. Lett.* **2001**, *87*, 098101, 1 – 4; A. Neiman, L. Schimansky-Geier, A. Cornell-Bell, F. Moss, *Phys. Rev. Lett.* **1999**, *83*, 4896 – 4899; J. F. Lindner, S. Chandramouli, A. R. Bulsara, M. Löcher, W. L. Ditto, *Phys. Rev. Lett.* **1998**, *81*, 5048 – 5051.

Rovibrational Corrections to Transition Metal NMR Shielding Constants

Michael Bühl,*[a] Petra Imhof,[a, b] and Michal Repisky[c]

Dedicated to Prof. Dr. W. Kutzelnigg
on the occasion of his 70th birthday.

Introduction

The development of theoretical tools to calculate NMR properties continues unabated.[1] A current focal point is to go beyond the treatment of molecules as vibrationless entities at 0 K and to account for the effect of vibrational averaging on chemical shifts or spin–spin coupling constants. Procedures have been devised to include rovibrational effects in the NMR calculation, for

[a] *Priv.-Doz. Dr. M. Bühl, Dr. P. Imhof*
     Max-Planck-Institut für Kohlenforschung
     Kaiser-Wilhelm-Platz 1
     45470 Mülheim an der Ruhr (Germany)
     Fax: (+ 49) 208-306 2996
     E-mail: buehl@mpi-muelheim.mpg.de

[b] *Dr. P. Imhof*
     Curent address:
     Interdisziplinäres Zentrum für Wissenschaftliches Rechnen
     Universität Heidelberg
     Im Neuenheimer Feld 368, 69120 Heidelberg (Germany)

[c] *M. Repisky*
     Institute of Inorganic Chemistry, Slovak Academy of Sciences
     Dubravska cesta 9, 84236 Bratislava (Slovak Republic)

     Supporting information for this article is available on the WWW under http://www.chemphyschem.org or from the author.

instance, by suitable perturbational treatments[2] or by approximating full or partial solutions of the nuclear Schrödinger equation.[3] The modeling of these effects by averaging chemical shifts over trajectories from classical molecular dynamics (MD) simulations is enjoying some popularity,[4, 5, 6] partly because these simulations can readily be extended to explicitly include a solvent.

We have used the latter approach to calculate thermal and solvent effects on the chemical shifts of transition metals.[6] Since the corresponding magnetic shielding constants can be quite sensitive to geometrical parameters,[7] pronounced rovibrational effects may be expected. In fact, large such effects, amounting to several hundreds of parts per million, were modeled for $\sigma(^{57}Fe)$ of some iron complexes, but smaller variations, on the order of a few dozen parts per million, were found for $\sigma(^{51}V)$ and $\sigma(^{55}Mn)$ in vanadate complexes and permanganate ion, respectively.[6]

Quantities averaged over classical MD trajectories do not include zero-point effects, which are purely quantum-mechanical in nature. For magnetic shieldings of lighter nuclei, these zero-point effects can be much larger than the thermal effects superimposed on them.[2, 3] We argued[6c,d] that thermal effects on transition-metal magnetic shieldings, evaluated from classical MD, should at least show the correct qualitative trend, since both classical and quantum-mechanical averaging would tend to increase the metal–ligand bond lengths with respect to their equilibrium values, and it is typically these distances that dominate the metal shieldings.[7b] To test this reasoning, we now report rigorous rovibrational corrections to shieldings of some typical transition metal complexes, evaluated perturbationally according to the procedure from ref. [2]

Results and Discussion

For our purpose, we adapted the corresponding implementation from the Dalton program package[8] such that energies, energy derivatives, and properties produced with another quantum chemistry code can be processed (specifically, from Gaussian 98[9]). This was necessary since at the beginning of this project the latest version of Dalton did not allow for DFT-based electronic-structure calculations, the method of choice for structures and properties of transition metal complexes.[10]

Briefly, the procedure consists of two parts: First, an effective geometry r_{eff} is constructed from the equilibrium geometry r_e, the harmonic frequencies ω_e, and the cubic force field $V^{(3)}$ [Eq. (1)].[11]

$$r_{\text{eff},j} = r_{\text{e},j} - \frac{1}{4\omega_{\text{e},j}^2} \sum_m \frac{V_{\text{e},jmm}^{(3)}}{\omega_{\text{e},m}} \tag{1}$$

Second, the magnetic shielding hypersurface $\sigma(r)$ is expanded around this effective geometry, and the vibrationally averaged σ_0 is calculated from $\sigma_{eff} = \sigma(r_{eff})$, the second derivative of the shielding surface $\sigma^{(2)}$, and the harmonic frequencies ω, all evaluated at r_{eff} [Eq. (2)],[2]

$$\sigma_0 = \sigma_{\text{eff}} + \frac{1}{4} \sum_i \frac{\sigma_{\text{eff},ii}^{(2)}}{\omega_{\text{eff},i}} \tag{2}$$